

Backstepping/DTC control of a double star synchronous machine drive

D. BOUDANA, L. NEZLI, A. TLEMÇANI, M.O. MAHMOUDI, M. DJEMAI and M. TADJINE

Direct torque control (DTC) allows for very high quality torque control without a need for current controllers tuning or using coordinate transformation. However, large torque ripples arise as well as inconstant inverter switching frequency due to the hysteresis of comparators. This paper presents a backstepping/DTC control based on the space vector modulation (SVPWM) for double star synchronous machine (DSSM) to reduce the torque, flux, current and speed pulsations during steady state. By the coordinate transformation the DSSM models are presented in view of control. Then a conventional DTC is developed to get a decoupled system and a PI controller is designed to control the speed. To improve the static and dynamic control performance of the DSSM, the speed controller is designed using a backstepping/DTC procedure in conjunction with SVPWM. Simulation results with the conventional DTC and proposed backstepping/DTC are presented and compared. Results show the effectiveness and the robustness of the approach proposed.

Key words: double star synchronous machine, direct torque control, backstepping/DTC, space vector modulation, robustness

1. Introduction

In the high power range, the synchronous machines are particularly attractive. For instance, the synchronous motor fed by current converter with intermediate DC-link are widely used in industrial adjustable speed drives. They operate in the same way as DC motors. However, the stator current presents a large harmonic, and consequently, cause high torque oscillations [1],[2].

With the development of high power semi conductor devices, synchronous machines are supplied by voltage source inverter. But the limitations on the gate-turn-off lead to the high current and torque ripple. To overcome this problem, synchronous machine is fed by multilevel inverter. Another way is application of the power segmentation on both inverter and machine. The most common structure uses double star synchronous machine whose windings are spatially phase shifted by 30 electrical degrees, supplied with source

D. Boudana, L. Nezli, A. Tlemçani, M.O. Mahmoudi and M. Tadjine are with LCP, ENP, 10 av. Pasteur, Hassen Badi, 16200 El Harrach, Alger, Algeria. M. Djemai is with ECS, ENSEA, 6 av. du Ponceau, 95014 Cergy-Pontoise Cedex, France. Corresponding author is A. Tlemçani, e-mail: h.tlemceni@yahoo.fr

Received 14.04.2008.

voltage inverters [3],[4]. Double star synchronous machine possesses several advantages over conventional three phase machine. This includes: increasing the inverter output power, reducing the amplitude of torque ripple, lowering the dc link current harmonics and improving the reliability, enabling of the the motor start and run even the loss of one or more phases [5].

Several methods have been proposed for the control of DSSM [6],[7],[8]. Complexity and parameters sensitivity are the most important disadvantages of these methods. An alternative solution is the use of direct torque control strategies [9]. The principle of conventional DTC is to select stator voltage vectors, according to the differences between the stator flux linkage and torque and their references, to keep stator flux and torque within the limits of two hysteresis bands. DTC allows for decoupling of the control of flux and torque without a need of coordinate transformation, PWM pulse generation and current regulation [10],[11]. The DTC has many advantages such as lower machine parameter dependence, fast torque response, elimination of d-q axes and rotor position sensor. However, the presence of hysteresis of the controllers leads to significant torque, flux and current pulsations and non-constant switching frequency operation. Otherwise, backstepping control is a newly developed technique for the control of uncertain non-linear systems, particularly systems which do not satisfy matching conditions. The most appealing point is to use the virtual control variable to make the original high-order system simple, thus the final control outputs can be derived step by step through suitable Lyapunov functions [12]. The application of this new technique in association with the DTC gives a new structure which allows for reducing the torque ripple and fixing the switching frequency.

In this paper, we propose a novel and simple backstepping/DTC strategy for double star synchronous machine to reduce the flux and torque ripple, and also to keep fixed switching frequency. The objective of the proposed control strategy is to replace the hysteresis controllers used in the conventional DTC by a backstepping/DTC strategy control in conjunction with SVPWM techniques. The proposed approach is verified and compared with the conventional DTC by simulation experiments.

2. Formulation of the problem

The stator voltage equation for DSSM is given by:

$$[v_s] = [R_s] [i_s] + \frac{d}{dt} ([L_{ss}] [i_s] + [M_{sr}] i_f) \quad (1)$$

with

$$[v_s] = [v_{a1} \ v_{a2} \ v_{b1} \ v_{b2} \ v_{c1} \ v_{c2}]^T \quad (2)$$

$$[i_s] = [i_{a1} \ i_{a2} \ i_{b1} \ i_{b2} \ i_{c1} \ i_{c2}]^T. \quad (3)$$

The original six dimensional system of the machine can be expressed in the rotor flux reference frame d-q plan as follows:

$$\begin{cases} v_d = R_s i_d + L_d \frac{di_d}{dt} - \omega L_d i_q \\ v_q = R_s i_q + L_d \frac{di_q}{dt} + \omega L_d i_d + \omega \phi_r \end{cases} \quad (4)$$

The electromagnetic torque equation is:

$$T_e = P (\phi_d i_q - \phi_q i_d) \quad (5)$$

with

$$\phi_r = M_d i_f$$

and rotating speed of rotor flux linkage

$$\phi_d = L_d i_d + \phi_r, \quad \phi_q = L_d i_q. \quad (6)$$

In order to control directly and independently the flux and the torque the model of the DSSM is expressed in the stator flux reference frame by using the transformation, which transforms variable in the rotor flux reference frame (d-q) to the stator flux reference frame x-y sa follows (Fig. 1):

$$\begin{bmatrix} \cos \delta & \sin \delta \\ -\sin \delta & \cos \delta \end{bmatrix} \quad (7)$$

The electrical equations for the DSSM in x-y reference frame are as follows [15]:

$$\begin{cases} v_x = R_s i_x - \omega_s L_d i_y + L_d \frac{di_x}{dt} + \omega \phi_r \sin \delta \\ v_y = R_s i_y + \omega_s L_d i_x + L_d \frac{di_y}{dt} + \omega \phi_r \cos \delta \end{cases} \quad (8)$$

where: ω_s is the rotating speed of stator flux linkage and δ is the angle between rotor and stator flux linkage.

The fluxes and the torque are given by:

$$\begin{cases} \phi_x = \phi_s = L_d i_x + \phi_r \cos \delta \\ \phi_y = 0 = L_d i_y - \phi_r \sin \delta \\ T_e = P \phi_s i_y \end{cases} \quad (9)$$

From (8) and (9) the model for the DSSM can be written as follows:

$$\begin{cases} \frac{di_y}{dt} = f_1 + b v_y \\ \frac{d\phi_s}{dt} = f_2 + v_x \\ j \frac{dw}{dt} = T_e - T_r \end{cases} \quad (10)$$

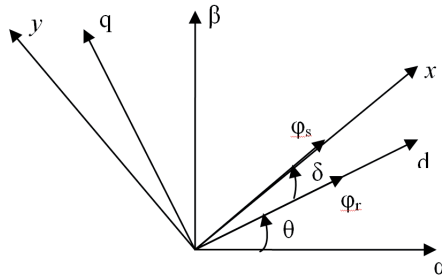


Figure 1. The stator and rotor flux linkages in different reference frames.

where

$$\begin{cases} f_1 = -\frac{1}{L_d} (R_s i_y + w_s \phi_s + (w_s - w) \phi_r \cos \delta) \\ f_2 = -\frac{R_s}{L_d} (\phi_s - \phi_r \cos \delta) \\ b = \frac{1}{L_d}. \end{cases} \quad (11)$$

The considered DSSM problem is to get a decoupling system between flux and torque and to track a desired reference for the speed. To do this, the control law is designed using the backstepping methodology together with a DTC structure. The equation of dynamics (10) allows for the following conclusions:

1. The speed can be controlled using the torque.
2. The flux can be controlled directly using the real control signal v_x .
3. The torque can be controlled directly using the real control signal v_y .

3. Direct Torque control of DSSM

The instantaneous electromagnetic torque T_e of DSSM is expressed as:

$$T_e = \frac{1}{L_d} P \phi_s \phi_r \sin(\delta). \quad (12)$$

It can be seen that T_e can be controlled by keeping the amplitude of the stator flux linkage constant and controlling the angle between the stator and rotor flux linkage. In DTC control, the stator flux linkage and the torque are directly controlled, using torque hysteresis controller and flux hysteresis controller to set the output voltage vector of inverter (Fig. 2).

$$T_e = P (\phi_\alpha i_\beta - \phi_\beta i_\alpha) \tag{16}$$

where

$$\begin{bmatrix} F_\alpha & F_\beta & F_{z1} & F_{z2} & F_{z3} & F_{z4} \end{bmatrix}^T = [T_s] [F_s], \tag{17}$$

F_s is voltage, courant or flux and

$$[T_s] = \frac{1}{\sqrt{3}} \begin{bmatrix} \cos(0) & \cos(\gamma) & \cos(\frac{2\pi}{3}) & \cos(\frac{2\pi}{3} + \gamma) & \cos(\frac{4\pi}{3}) & \cos(\frac{4\pi}{3} + \gamma) \\ \sin(0) & \sin(\gamma) & \sin(\frac{2\pi}{3}) & \sin(\frac{2\pi}{3} + \gamma) & \sin(\frac{4\pi}{3}) & \sin(\frac{4\pi}{3} + \gamma) \\ \cos(0) & \cos(\pi - \gamma) & \cos(\frac{4\pi}{3}) & \cos(\frac{\pi}{3} - \gamma) & \cos(\frac{2\pi}{3}) & \cos(\frac{5\pi}{3} - \gamma) \\ \sin(0) & \sin(\pi - \gamma) & \sin(\frac{4\pi}{3}) & \sin(\frac{\pi}{3} - \gamma) & \sin(\frac{2\pi}{3}) & \sin(\frac{5\pi}{3} - \gamma) \\ 1 & 0 & 1 & 0 & 1 & 0 \\ 0 & 1 & 0 & 1 & 0 & 1 \end{bmatrix}. \tag{18}$$

4. Selection of voltage vectors

The DSSM is supplied with two VSIs. Each inverter can be controlled independently. However, if we consider the two inverters as a six-phase voltage source inverter we obtain a total of 64 switching modes. By using the transformation matrix (18) the 64 voltage vectors corresponding to the switching modes are projected on three planes. From 64 vectors there are only 12 voltage vectors that offer a maximum voltage on the $\alpha - \beta$ plane and keep the harmonics on the $Z_1 Z_2$ plane at a minimum [5],[14],[18].

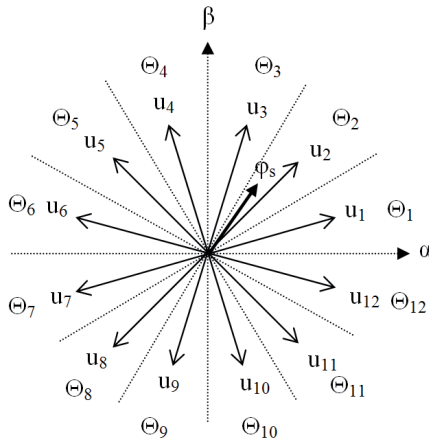


Figure 3. The chosen inverter voltage vectors projected on $\alpha - \beta$ plane.

The voltage vector plane is divided into twelve sectors so that each voltage vector divides each region into two equal parts as shown in Fig. 3. In each sector, four of the

Table 4. The switching states for inverters

Φ	$\tau \setminus \Theta$	Θ_1	Θ_2	Θ_3	Θ_4	Θ_5	Θ_6	Θ_7	Θ_8	Θ_9	Θ_{10}	Θ_{11}	Θ_{12}
$\Phi = 1$	$\tau = 1$	u_3	u_4	u_5	u_6	u_7	u_8	u_9	u_{10}	u_{11}	u_{12}	u_1	u_2
	$\tau = 0$	u_{11}	u_{12}	u_1	u_2	u_3	u_4	u_5	u_6	u_7	u_8	u_9	u_{10}
$\Phi = 0$	$\tau = 1$	u_5	u_6	u_7	u_8	u_9	u_{10}	u_{11}	u_{12}	u_1	u_2	u_3	u_4
	$\tau = 0$	u_9	u_{10}	u_{11}	u_{12}	u_1	u_2	u_3	u_4	u_5	u_6	u_7	u_8

twelve voltage vectors may be used. The switching table used in this work is indicated in Tab. 1. The output of the flux hysteresis comparator is denoted as Φ , the output of the torque hysteresis comparator is denoted as τ . The flux hysteresis comparator is a two valued comparator. $\Phi = 1$ means that the actual value of the amplitude of the flux linkage is below the reference value and $\Phi = 0$ means that the actual value is above the reference value. The same is true for the torque.

5. Proposed backstepping/DTC for DSSM

The proposed backstepping/DTC control retains the advantages of the conventional DTC. In fact, instead of the hysteresis controllers a backstepping/DTC control is used for the speed of the DSSM to track the reference speed and get decoupling between stator flux linkage and torque (Fig. 4).

Let $e_w = w - w^*$, $e_\phi = \phi - \phi^*$ and $e_T = T - T^*$. The following result can be established.

Proposition Consider the DSSM plant model (10). Let the backstepping/DTC controllers be:

$$\begin{cases} v_x = -f_2 + \dot{\phi}_s^* - k_2(\phi_s - \phi_s^*) \\ v_y = \frac{-1}{pb\phi_s} [p\phi_s f_1 + k_1(T_e - T_e^*) + (w - w^*) + p\dot{\phi}_s i_y - \dot{T}_e^*] \\ T_e^* = j\dot{w}^* - k_3(w - w^*) - k_4 \text{sign}(w - w^*) \end{cases} \quad (19)$$

where $k_1, k_2, k_3 > 0$ and $k_4 > \max(T_r)$, $\phi_s \neq 0$. Then e_w , e_ϕ and e_T are asymptotically stable.

Proof The proof is based on two steps using the backstepping/DTC approach.

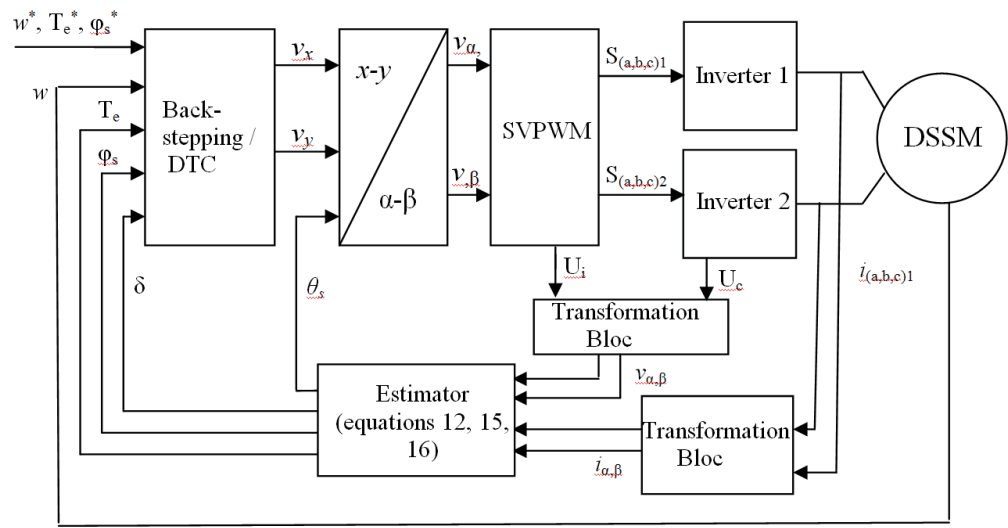


Figure 4. Proposed Backstepping /DTC scheme for DSSM.

Step 1

Consider the following Lyapunov function related to the speed dynamic defined in (10):

$$\left\{ V_1 = \frac{1}{2}j(w - w^*)^2 > 0. \right. \tag{20}$$

This function is globally positive definite over the whole state space. Its derivative is given by:

$$\dot{V}_1 = j(w - w^*)(\dot{w} - \dot{w}^*) = (w - w^*)(T_e - T_r - j\dot{w}^*). \tag{21}$$

If it is supposed that $T_e \rightarrow T_e^*$, we obtain

$$\dot{V}_1 = -k_3(w - w^*)^2 - (w - w^*)[-k_4 \text{sign}(w - w^*) - T_r] \tag{22}$$

The term: $(w - w^*)[-k_4 \text{sign}(w - w^*) - T_r] < 0; \forall (w - w^*)$ and $\forall T_r$ than

$$\dot{V}_1 < -k_3(w - w^*)^2 < 0. \tag{23}$$

This means that w converge exponentially to w^* . Hence if T_e is forced to take the desired value T_e^* , the speed tracking error tends to zero.

Step 2

The objective of this step is to establish the control voltage v_x that impose ϕ_s to acquire the desired value ϕ_s^* and the control voltage v_y that impose T_e to acquire the desired value T_e^* . Consider the augmented Lyapunov function:

$$V_2 = V_1 + \frac{1}{2}(\phi - \phi^*)^2 + \frac{1}{2}(T_e - T_e^*)^2 > 0. \tag{24}$$

Its time derivative is expressed by:

$$\dot{V}_2 = \dot{V}_1 + (\phi_s - \phi_s^*) (\dot{\phi}_s - \dot{\phi}_s^*) + (T_e - T_e^*) (\dot{T}_e - \dot{T}_e^*). \quad (25)$$

Recall that:

$$\dot{V}_1 = (w - w^*) (T_e - T_r - j\dot{w}^*) = (w - w^*) (T_e - T_e^*) + (w - w^*) (T_e^* - T_r - j\dot{w}^*) \quad (26)$$

Replacing T_e^* by its value from (19), we obtain:

$$(w - w^*) (T_e - T_e^*) + (w - w^*) (T_e^* - T_r - j\dot{w}^*) \leq (w - w^*) (T_e - T_e^*) - k_3 (w - w^*)^2. \quad (27)$$

The derivative of the Lyapunov function (25) becomes:

$$\dot{V}_2 \leq (w - w^*) (T_e - T_e^*) - k_3 (w - w^*)^2 + (\phi_s - \phi_s^*) (\dot{\phi}_s - \dot{\phi}_s^*) + (T_e - T_e^*) (\dot{T}_e - \dot{T}_e^*). \quad (28)$$

The torque and the flux are given by (11) and their derivatives are:

$$\begin{cases} \dot{T}_e = p\dot{\phi}_s i_y + p\phi_s \dot{i}_y \\ \dot{i}_y = f_1 + b v_y \\ \dot{\phi}_s = f_2 + v_x. \end{cases} \quad (29)$$

Replacing the control law (19) in (29), equation (28) becomes:

$$\dot{V}_2 \leq -k_3 (w - w^*)^2 - k_2 (\phi_s - \phi_s^*)^2 - k_1 (T_e - T_e^*)^2 < 0. \quad (30)$$

Hence using the Lyapunov theorem, we conclude that:

$$\begin{cases} \lim_{t \rightarrow +\infty} (w - w^*) = 0 \\ \lim_{t \rightarrow +\infty} (\phi_s - \phi_s^*) = 0 \\ \lim_{t \rightarrow +\infty} (T_e - T_e^*) = 0. \end{cases} \quad (31)$$

That is, the tracking errors are asymptotically stable. \square

6. Space vector PWM

The presence of hysteresis controllers in the conventional DTC strategy produces varying switching frequency during operation of the inverters. But the space vector PWM control allows for operating in the constant switching frequency. The objective of SVPWM control is to approximate the reference voltage vector instantaneously by combination of switching states corresponding to the basic space vectors. During each sampling period T_s , a set of five voltage vectors are chosen to synthesize the $\alpha - \beta$ voltages

vectors and to maintain the average volt-seconds Z_1 Z_2 planes to be zero. The SVPWM strategy is accomplished by the following equations [5],[14]:

$$\begin{bmatrix} T_{n-2} \\ T_{n-1} \\ T_n \\ T_{n+1} \end{bmatrix} = \begin{bmatrix} v_{\alpha}^{n-2} & v_{\alpha}^{n-1} & v_{\alpha}^n & v_{\alpha}^{n+1} \\ v_{\beta}^{n-2} & v_{\beta}^{n-1} & v_{\beta}^n & v_{\beta}^{n+1} \\ v_{z1}^{n-2} & v_{z1}^{n-1} & v_{z1}^n & v_{z1}^{n+1} \\ v_{z2}^{n-2} & v_{z2}^{n-1} & v_{z2}^n & v_{z2}^{n+1} \end{bmatrix}^{-1} \begin{bmatrix} v_{\alpha}^* T_s \\ v_{\beta}^* T_s \\ 0 \\ 0 \end{bmatrix} \tag{32}$$

$$T_0 = T_s - (T_{n+1} + T_n + T_{n-1} + T_{n-2}) \tag{33}$$

where v_x^k is the projection of the k th voltage vector on the x axis and T_k is the dwell time of that vector during time interval T_s . The quantities v_{α}^* and v_{β}^* are the $\alpha - \beta$ plane reference voltages (Fig. 5). At any PWM period, the applied sequence of adjacent vectors $v_{n-2}, v_{n-1}, v_n, v_{n+1}$ and the zero vector v_0 are $v_0 - v_{n-2} - v_{n-1} - v_n - v_{n+1} - v_0 - v_{n+1} - v_n - v_{n-1} - v_{n-2} - v_0$ and the respective durations are:

$$\frac{T_0}{4}, \frac{T_{n-2}}{2}, \frac{T_{n-1}}{2}, \frac{T_n}{2}, \frac{T_{n+1}}{2}, \frac{T_0}{2}, \frac{T_{n+1}}{2}, \frac{T_n}{2}, \frac{T_{n-1}}{2}, \frac{T_{n-2}}{2}, \frac{T_0}{4}$$

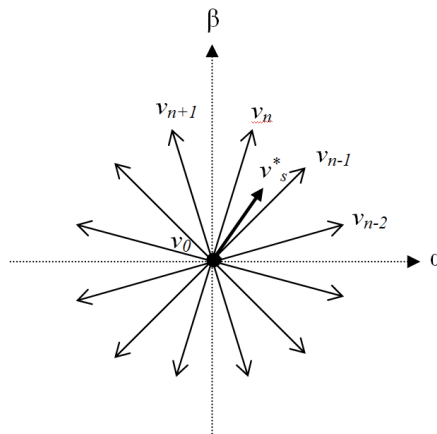


Figure 5. The applied sequence of adjacent vectors.

7. Comparative study

In this section, we aim to compare our proposed scheme to the conventional DTC for DSSM. We consider three situations:

Situation 1: Step change in torque.

For backstepping/DTC and conventional DTC for DSSM we have imposed a reference torque 10 [Nm] at time 0.2 [ms]. Fig. 7 and 8 present obtained results. We can see, that both control approaches ensure good flux linkage and torque tracking. Furthermore, both methods of control allow for exact decoupling between stator flux linkage and torque. However, the backstepping/DTC for DSSM decreases considerably the torque ripple and provides faster torque response.

Situation 2: Speed tracking.

To test the speed tracking we have simulated both control approaches:

- a. Fig. 9 and 10: speed step response of amplitude 100 [rd/s] with load torque $T_r = 8$ [Nm] applied at time $t = 1$ [sec].
- b. Fig. 11 and 12: speed square step response of amplitude 100 [rd/s] with the machine not loaded.

In both control approaches a torque limiter was introduced in order to limit the produced torque to the value 10 [Nm]. It can be observed, that with both, PI speed controller and backstepping/DTC speed controller, the speed track its reference and the rejection of disturbance is immediate.

Situation 2: Stator resistance variation.

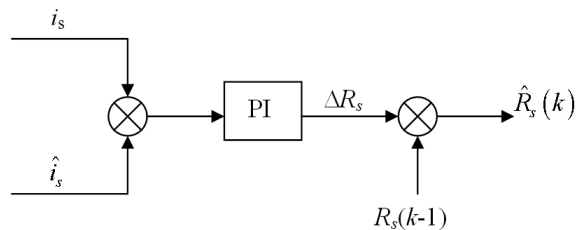
For both DTC control schemes we have simulated variation of stator resistance as shown in Fig. 15. The obtained results, shown in Fig. 13 and 14, show that the torque and flux are oscillating when stator resistance is increased. Thus incorrect resistance stator can cause instability. To overcome this problem we used the stator resistance estimator shown in Fig. 6. The error in the stator current is used as an input to the PI estimator. The output of the PI estimator is continuously added to the previously estimated stator resistance.

Fig. 15,16 and 17 show the actual and estimated stator resistance and their error, respectively. In Fig. 18 and 19 we have inserted the estimated stator resistance in control scheme. The obtained results are very satisfactory.

Table 2 summarizes the results of the comparative study. From this results one can conclude, that for the DSSM, the backstepping/DTC is significantly better than the conventional DTC.

Table 5. Comparative study between backstepping/DTC and conventional DTC for DSSM.

	Torque ripple	Response time	Speed response	Stator resistance variation
Backstepping/DTC	1.3 %	5 [ms]	- Good tracking - Good decoupling - Rejection of disturbance	Unstable
Conventional DTC	2.4 %	10 [ms]	- Good tracking - Exact decoupling - Rejection of disturbance	Unstable

Figure 6. Block diagram of the stator resistance estimator (\hat{i}_s is the estimated stator current).

8. Conclusion

In this paper, backstepping/DTC method for DSSM is presented based on voltage space vector modulation. The proposed method reduces the torque/flux ripples and preserves the advantages of the conventional DTC. The use of SVPWM to assure the DSSM voltage demand in the proposed method allows for operating at the constant and controllable switching frequency. In conventional DTC a single voltage vector is applied during sampling time. In backstepping/DTC-SVPWM a sequence of six vectors is applied during the same time. Simulations results verify the effectiveness of the backstepping/DTC-SVPWM control both in dynamic and static performances.

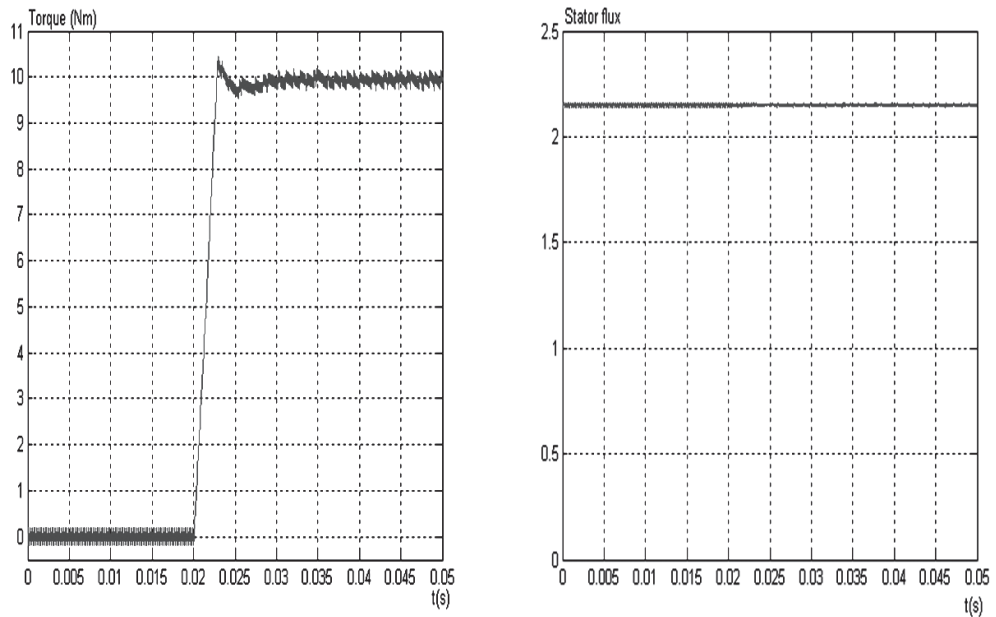


Figure 7. Performance of conventional DSSM DTC for situation 1.

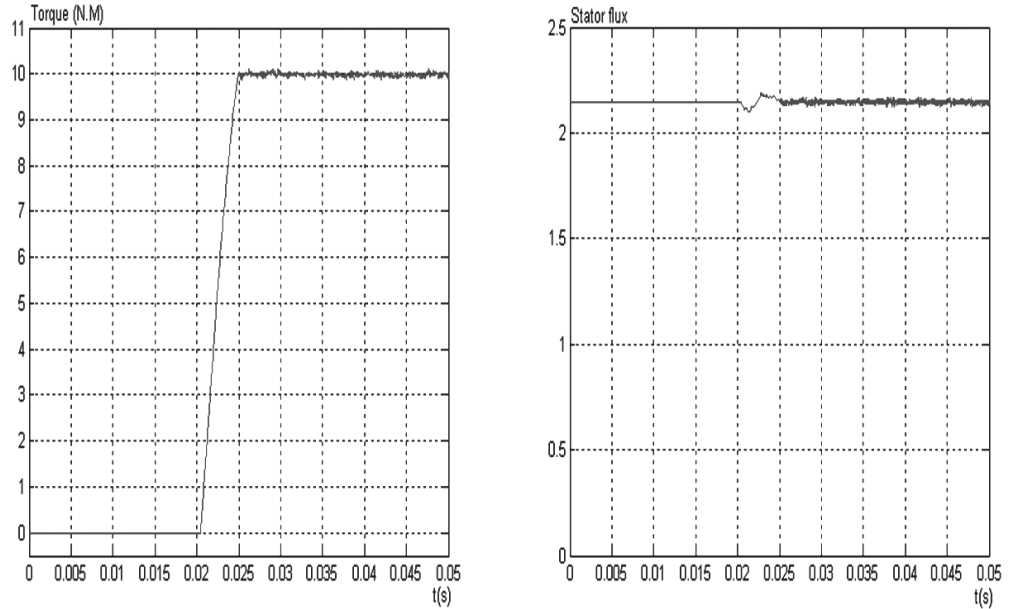


Figure 8. Performance of backstepping/DTC control of DSSM for situation 1.

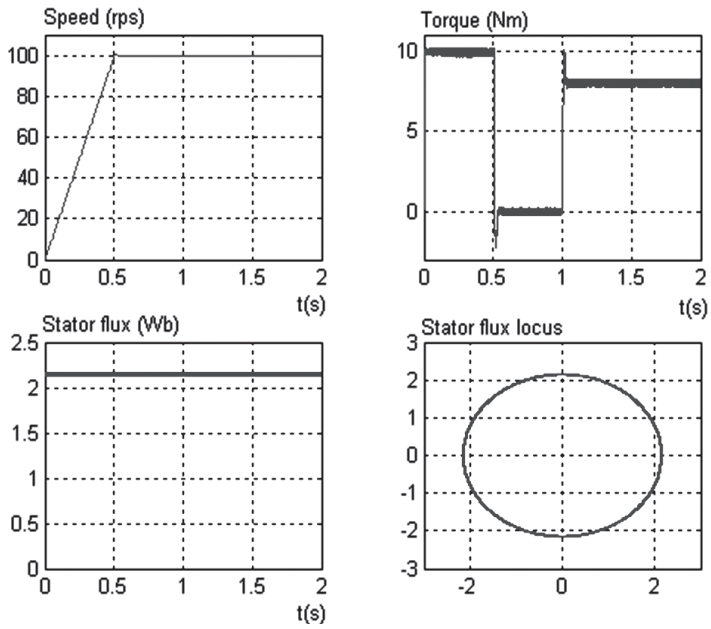


Figure 9. Performance of conventional DSSM DTC for situation 2-a.

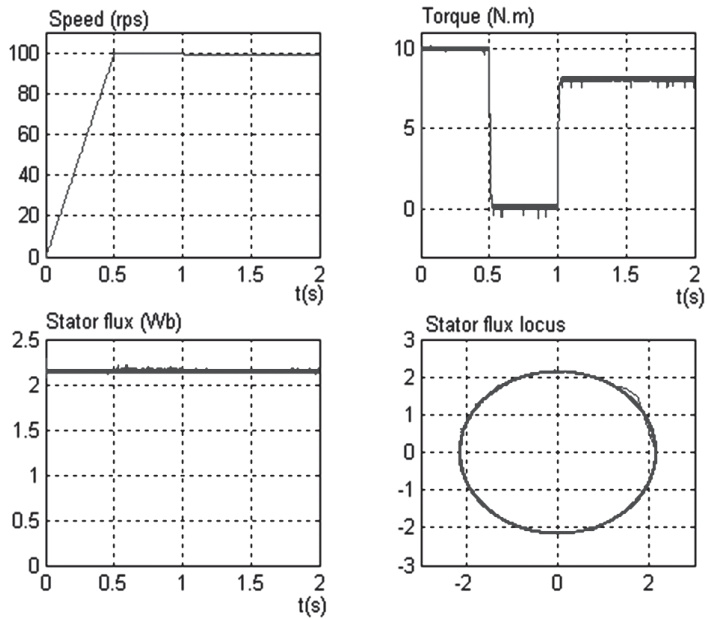


Figure 10. Performance of backstepping/DTC control of DSSM for situation 2-a.

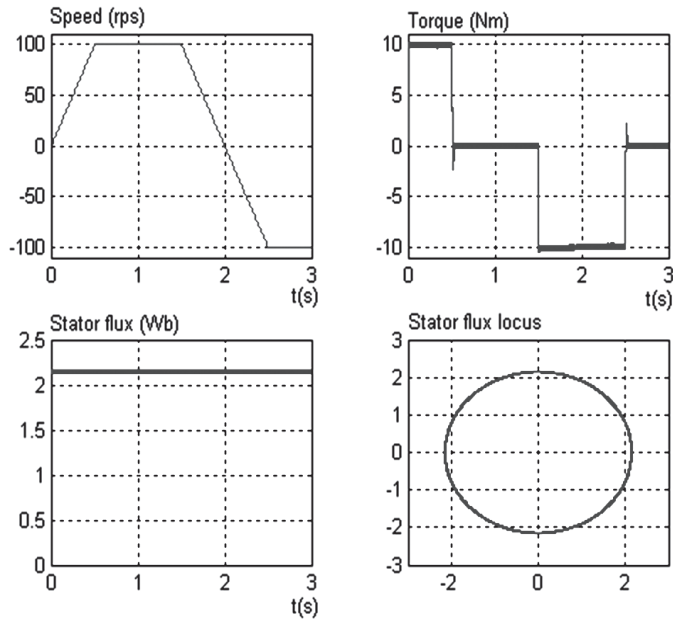


Figure 11. Performance of conventional DSSM DTC for situation 2-b.

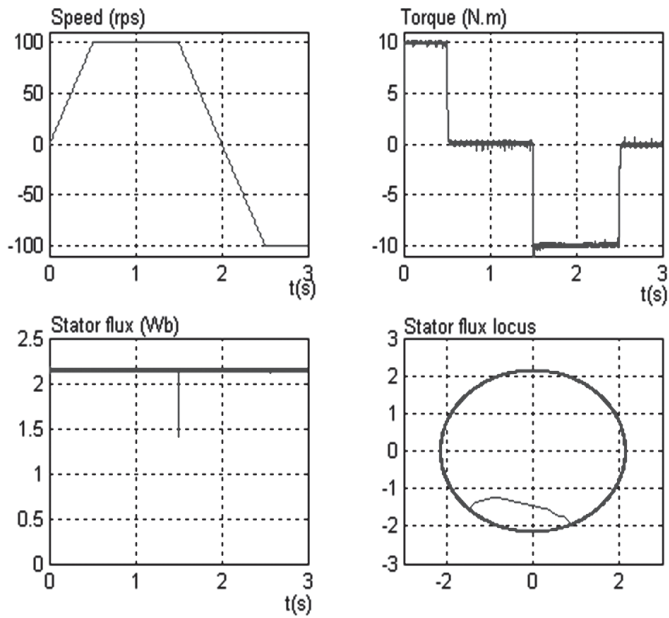


Figure 12. Performance of backstepping/DTC control of DSSM for situation 2-b.

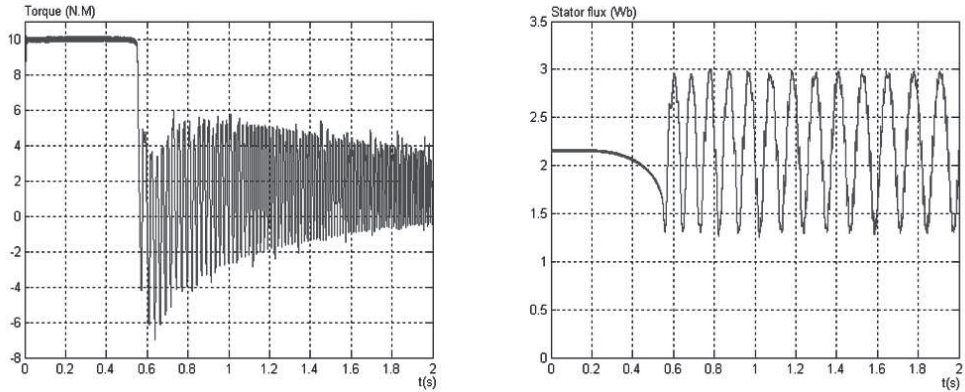


Figure 13. The resistance variation effect for conventional DTC control of DSSM.

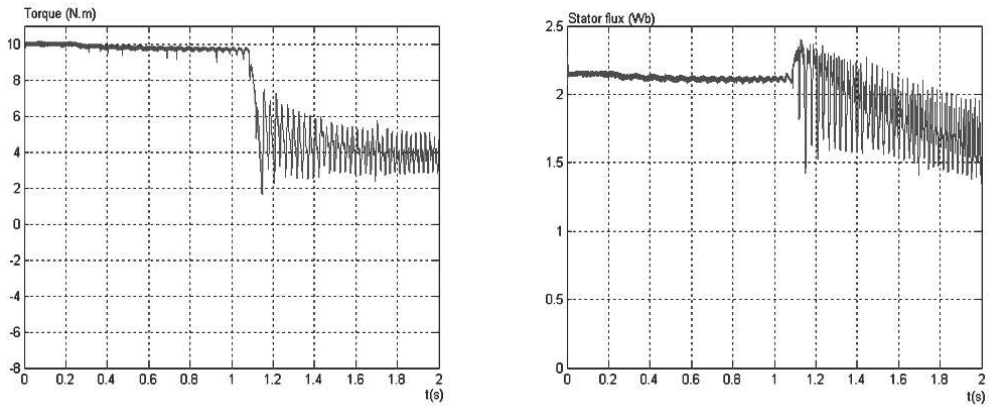


Figure 14. The resistance variation effect for backstepping/DTC control of DSSM.

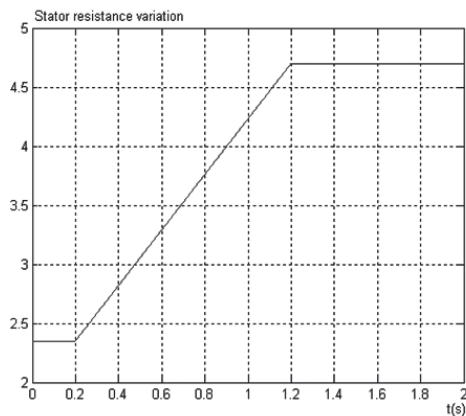


Figure 15. Actual stator resistance variation.

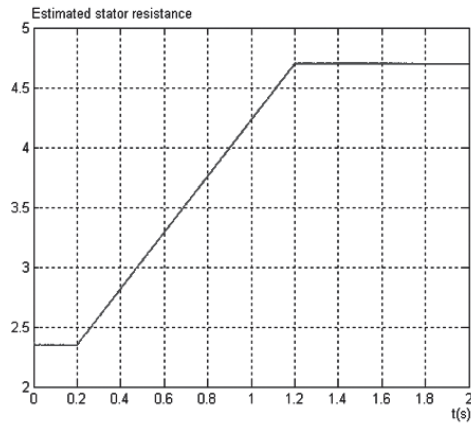


Figure 16. Estimated stator resistance.

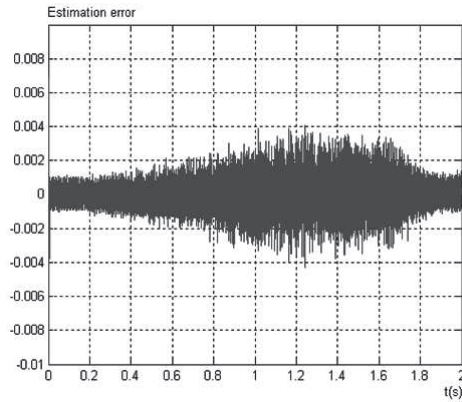


Figure 17. Estimation error.

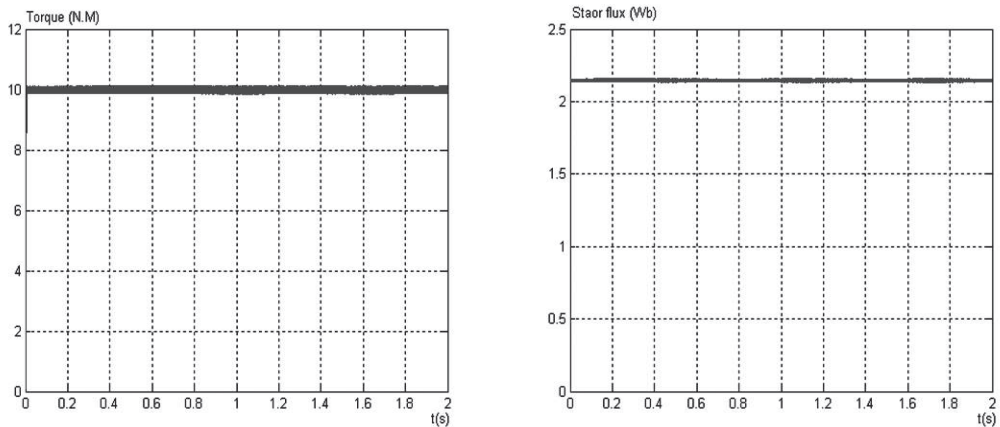


Figure 18. Performance of conventional DSSM DTC with estimated stator resistance.

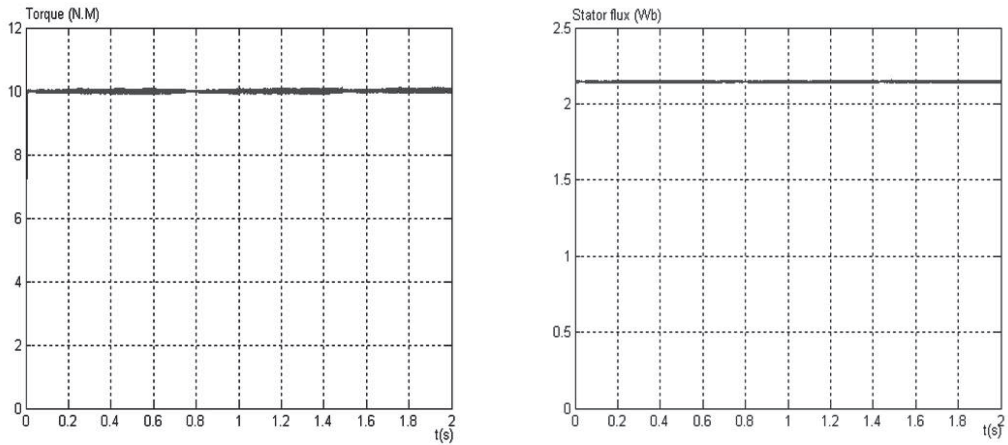


Figure 19. Performance of backstepping/DTC control of DSSM with estimated stator resistance.

Appendix 1: List of principal symbols

i_{a1}, i_{a1}, i_{a1}	: stator current a, b, c phase of first winding
i_{a2}, i_{a2}, i_{a2}	: stator current a, b, c phase of second winding
i_{α}, i_{β}	: stator current $\alpha - \beta$ axis
i_x, i_y	: stator current x-y axis
i_s	: stator current vector
v_{a1}, v_{b1}, v_{c1}	: simple voltage of stator three phase first winding
v_{a2}, v_{b2}, v_{c2}	: simple voltage of stator three phase second winding
v_s	: stator voltage vector
v_d, v_q	: stator voltages d-q axis
v_{α}, v_{β}	: stator voltages $\alpha - \beta$ axis
v_x, v_y	: stator voltages x-y axis
L_d, L_q	: d-q inductances
$[L_{ss}]$: stator inductance matrix
$[M_{sr}]$: stator-rotor mutual inductance matrix
$[R_s]$: $\text{diag}(R_S R_S R_S R_S R_S R_S)$
R_s	: stator resistance
R_f	: rotor resistance
T_e, T_e^*	: electromagnetic torque, reference torque
T_r	: load torque
ϕ_s, ϕ_s^*	: stator flux vector, reference flux vector
ϕ_d, ϕ_q	: stator flux d-q axis
$\phi_{\alpha}, \phi_{\beta}$: stator flux $\alpha - \beta$ axis
ϕ_x, ϕ_y	: stator flux x-y axis
w	: rotating speed of rotor flux linkage

w_s	: rotating speed of stator flux linkage
Φ_i	: output of the flux hysteresis comparator
τ	: output of the torque hysteresis comparator
δ	: angle between rotor and stator flux linkage
θ_r, θ_s	: angle of rotor flux linkage, angle of stator flux linkage
Θ_i	: the region numbers for the stator linkage positions
E_T, E_ϕ	: torque error, flux error.
J	: moment of inertia
f_r	: friction coefficient
P	: number of pole pairs.

Appendix 2: DSSM parameters

$$\begin{aligned}
 P_n &= 5 \text{ [kW]} \\
 U_c &= 232 \text{ [V]} \\
 i_f &= 1 \text{ [A]} \\
 R_s &= 2.35 \ \Omega \\
 R_f &= 30.3 \ \Omega \\
 L_d &= 0.3811 \text{ [H]} \\
 L_f &= 15 \text{ [H]} \\
 M_d &= 2.146 \text{ [H]} \\
 J &= 0.05 \text{ [Nms}^2\text{/rd]} \\
 f_r &= 0.001 \text{ [Nms/rd]} \\
 P &= 1.
 \end{aligned}$$

References

- [1] L. WERREN: Synchronous machine with 2 three phase winding, spatially displaced by 30°EL. Commutation reactance and model for converter-performance simulation. *ICEM*, Lausanne (Switzerland), **2** (1984), 781-784.
- [2] N. MOUBAYED, F. MEIBODY-TABAR, B. DAVAT: Alimentation par deux onduleurs de tension d'une machine synchrone double étoile. *Revue Internationale de Génie Electrique (RIGE)*, **1**(4), (1998), 457-470, (in French).
- [3] P.C. SEN: Electric motor drives and control - past present and future. *IEEE Trans. on Industrial Electronics*, **37**(6), (1990), 562-575.
- [4] Z. CHEN and A.C. WILLIAMSON: Simulation study of a double three phase electric machine. *Proc. Int. Conf. on Electric Ship*, Istanbul, Turkey, (1998), 215-220.

- [5] D. HADIOUCHE, H. RAZIK and A. REZZOUG: Modeling on double star induction motor for space vector PWM control. *ICEM 2000*, Finland, **1** (2000), 392-396.
- [6] L. NEZLI, M.O. MAHMOUDI, M.S. BOUCHERIT and M.DJEMAI: On vector control of double star synchronous machine with current fed inverters. *The Mediterranean J. of Measurement and Control*, **1**(3), (2005).
- [7] F.TERRIEN: Commande d'une machine synchrone double étoile, alimentée par deux onduleurs MLI. Thèse de doctorat de l'université de Nantes, 2000, (in French).
- [8] M. MERABTENE: Modelisation dynamique et commande d'une machine synchrone double étoile, alimentée par des onduleurs MLI fonctionnement en mode normal et dégrade. Thèse de doctorat de l'université de Nantes, 2005, (in French).
- [9] R. BOJOI, F. FARINA, G. GRIVA, F. PROFUMO, A. TENCONI: Direct torque control for dual-three phase induction motor drives. *IEEE Trans. on Industry Applications*, **41**(6), (2005), 1627-1636.
- [10] C. LASCU, I. BOLDEA and F.BLAABJERG: A modified direct torque control for induction motor sensorless drive. *IEEE Trans. on Industry Applications*, **36**(1), (2000), 122-130.
- [11] L. TONG, L. ZONG and M.F. RAHMAN: Modeling and experimental approach of a novel direct torque control scheme for interior permanent magnet synchronous machine drive. *Proc.IEEE IECON'02*, **1** Seville, Spain, (2002), 235-240.
- [12] J.ZHOU and Y.WANG: Adaptative backstepping speed controller design for permanent magnet synchronous motor. *IEE Pro.-Electr. Power Appl.*, **149**(2), (2002).
- [13] M.F.BENKHORIS, M.MERABTENE, F.MEIBODY-TABAR, B.DAVAT, E.SEMAIL: Approches de modélisation de la machine synchrone double étoile alimente par des onduleurs de tension en vue de la commande. *RIGE*, **6**(5-6), (2003), 579-608, (in French).
- [14] Y. ZHAO and T.A. LIPO: Space vector PMW control of dual three-phase induction machine using vector space decomposition. *IEEE Trans. on Industry Applications*, **31**(5), (1995), 1100-1109.
- [15] L. ZONG, M.F. RAHMAN, W.Y. HU and K.W. LIM: A direct torque controller for permanent magnet synchronous motor drives. *IEEE Trans. on Energy Conversion*, **14**(3), (1999).
- [16] L. ZONG, M.F. RAHMAN, W.Y. HU and K.W. LIM: Analysis of direct torque control in permanent magnet synchronous motor drives. *IEEE Trans. Power Electronics*, **12**(3), (1997), 528-536.

-
- [17] G.S. BUJA and M.P. KAZMIERKOWSKI: Direct torque control of PWM inverter-fed AC motors-a survey. *IEEE Trans. on Industrial Electronics*, **51**(4), (2004), 744-757.
- [18] N.MADANI: Commande a structure variable d'une machine asynchrone double étoile alimentée par deux onduleurs MLI. Thèse de doctorat de l'université de Nantes, 2004, (in French).